Total AC Interferences Between a Power Line Subject to a Single-Phase Fault and a Nearby Pipeline with Multilayered Soil

Caio M. Moraes
Gustavo H. de Sá Matos *
Amauri G. Martins-Britto
Kleber M. Silva
Department of Electrical Engineering
University of Brasília, UnB
Brasília, Brazil
{moraes.caio@aluno., amaurigm@, klebermelo@}unb.br, gustavodesamatos@gmail.com*

***Abstract*—This paper describes the problem of electromagnetic interferences between power lines and metallic structures, caused by inductive and conductive coupling mechanisms, and the main risks to which personnel and facilities are exposed. An EMTP-based implementation is proposed to predict induced voltage levels on a target circuit, due to interferences caused by overhead power lines under steady-state nominal load as well as fault conditions, using generalized formulas to represent the N-layered soil. Results are tested by means of a case study of a real right-of-way shared and comparisons with results obtained using industry-standard software. Results show that the proposed method is accurate, with errors smaller than 8%. Stress voltage values in the interfered pipeline are the order of 50 kV, exposing the structure coating to risk of breakdown, which may lead to corrosion and pipeline failure. A mitigation is designed and proven to reduce voltage values to safe levels, in compliance with the nominal limits from the manufacturer.**

***Index Terms*—Electromagnetic interferences, Electromagnetic Transient Program (EMTP), pipelines, single-phase fault and TLs.**

I. Introduction

Due to the trend of sharing right-of-ways with other facilities, forming the so called utility corridors, and the energy levels involved, transmission lines (TLs) may induce currents in nearby metal structures that are not designed to conduct electricity. This effect may raise risks to metallic installations neighboring the TLs through three types of electromagnetic interference (EMI) mechanisms: inductive, conductive and capacitive couplings [1].

EMIs are influenced by current levels flowing through TL conductors, length of exposure, soil characteristics and constructive aspects of the facilities involved [1].

Serious design errors may occur if these EMI are not properly addressed, exposing personnel and installations to risks, which justifies the efforts in developing reliable and realistic simulation models.

EMI studies addressed in literature generally represent the soil as semi-infinite and homogeneous structure or represent N-layered soils by equivalent homogeneous models. This approach is reported to yield inaccuracies in a variety of practical cases, due to the multilayered characteristic of natural soils. Moreover, to the best of the author's knowledge, there is no report in the specialized EMI literature accounting for arbitrary multilayered soil models within the EMTP-based paradigm [2], [3], [4].

This paper presents an EMTP-based implementation for inductive and conductive coupling studies caused by a TL under nominal load and phase-to-ground fault conditions with multilayered soil models.

Self and mutual impedance calculations are based on a generalized solution for overhead and buried conductors considering N-layered soils, proposed by Tsimiatros et al [5].

To properly account for earth conduction effects, the generalized N-layered Green's function, proposed by He et al. [6] and Li et al. [7], is used to represent the ground potential rise along the interfered structure, due to currents flowing into the soil under fault conditions.

The proposed implementation is leveraged to analyze the case of a real right-of-way in Brazil, shared between a 138 kV TL and an underground metallic pipeline. A 3-layered soil model is determined from local resistivity measurements. The proposed method is used to calculate the resulting stress voltages due to a phase-to-ground fault.

The obtained results are compared with CDEGS and present NRMSD errors of less than 8% in the cases analyzed. Stress voltages in the pipeline coating reached values close to 50 kV, which subjects the installation to risks that must be addressed according to safety standards.

Then, further simulations are performed to design a mitigation solution to reduce stress voltage levels along the interfered pipeline, which is demonstrated to reduce the initial stress voltage approximately in 50%, thus ensuring compliance with industry standards.

II. Mathematical Model

A. Inductive coupling

Currents flowing in an energized conductor produces a time-varying magnetic field, as shown in Fig. 1. This time-varying magnetic field causes electromotive forces (EMFs) and its induces voltage and current on a metallic structure laid parallelly to the energized conductor. This electromagnetic phenomenon is known as inductive coupling [1].

The inductive influence of a transmission line conductor on a nearby pipeline depends on the current magnitude, distance between structures, exposure length, soil resistivity, as well as the characteristics of installations involved [1].

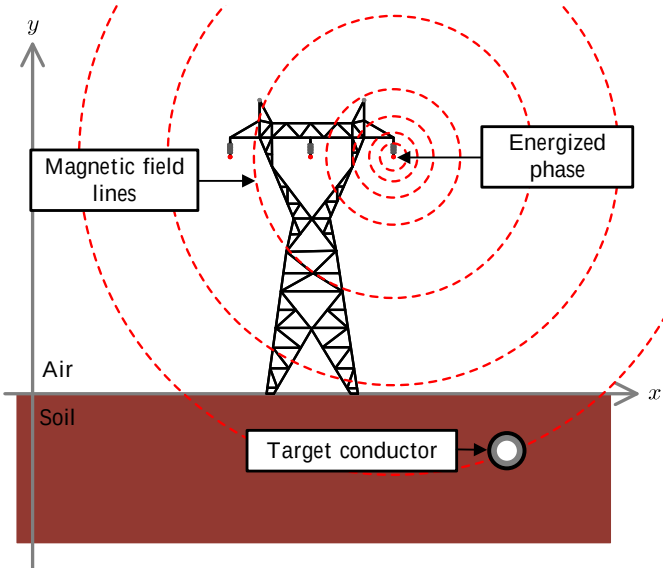

Fig. 1. Inductive coupling phenomenon, adapted from [12].

The induced EMF (E) is given by [1]:

$$E = Z_m \times I \tag{1}$$

in which Z_m is the mutual impedance matrix of system, in ohms.meter; I is the current in the energized conductor, in ampères; and E is the EMF in the target metallic structure, in volts per meter.

B. Mutual impedance for N-layered soil

The mutual impedance, described by each element of matrix Z_m, are calculated based on a generalized solution proposed by Tsiamitros et al. [5]. The generalized solution is a wide solution in comparison to the well-known Carson's [8], Nakagawa's [9] and Pollaczek's [10] formulas due to cover complex configurations composed of both overhead and buried conductors on N-layered earth.

Fig. 2 illustrates two conductors i and j in an N-layer earth structure, in each i^{th} earth layer has permeability (μ_i), permittivity (ϵ_i), conductivity (σ_i) and thickness (d_i). The conductors are assumed buried in the m^{th} and l^{th} layer of the N-layer earth, respectively. The per unit length mutual impedance $Z_{i,j}$, is calculated from (2), in which $\omega = 2\pi f$ is the angular velocity, in radians per seconds; h_1 and h_2 are relative height to superior layers m and l, respectively, in meters; $y_{i,j}$ is the horizontal distance between the conductor i and j, in meters; and $\bar{\alpha}_i = \sqrt{u^2 + \bar{\gamma}_i^2}$, $\bar{\gamma}_i^2 = j\omega\mu_i(\sigma_i + j\omega\epsilon_i)$, which $i = 0, 1, 2, \ldots, N$ [5].

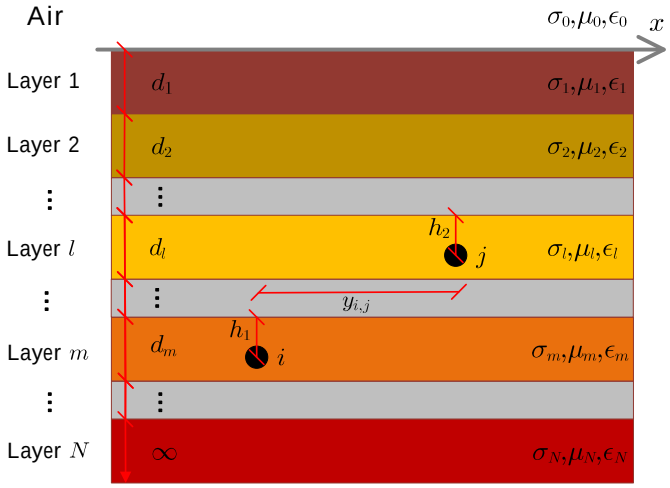

Fig. 2. Two underground conductors in N-layered soil.

The terms $D\bar{T}N_i$, $D\bar{T}D_i$, $T\bar{D}N_k$ and $T\bar{D}D_k$, given in (3)-(10), relate the electromagnetic and geometrical characteristics of the succendent layers, in which $i = 0, 1, 2, \ldots, N$ and $k = 0, 1, 2, \ldots, m$. The first letters of the terms TD ("Top to Down") and DT ("Down to Top") denotes the direction of the recursive formulas and the latter D ("Denominator") and N ("Numerator") denotes which usually appears the terms during the analysis [5].

$$\begin{aligned} D\bar{T}N_i = {} & (\mu_{i+1}\bar{\alpha}_i - \mu_i\bar{\alpha}_{i+1})D\bar{T}D_{i+1} \\ & + (\mu_{i+1}\bar{\alpha}_i + \mu_i\bar{\alpha}_{i+1})D\bar{T}N_{i+1}e^{-2\bar{\alpha}_{i+1}d_{i+1}}, \end{aligned} \tag{3}$$

$$\begin{aligned} Z_{i,j} &= \frac{j\omega\mu_m}{2\pi}\int_0^\infty \frac{cos(uy_{i,j})}{\bar{\alpha}_m} \times \left\{ 2^{m-l}\frac{(\mu_1\mu_2\ldots\mu_{m-1})(\bar{\alpha}_1\bar{\alpha}_2\ldots\bar{\alpha}_m)(e^{-\bar{\alpha}_l d_l}e^{-\bar{\alpha}_{l+1}d_{l+1}}\ldots e^{-\bar{\alpha}_m d_m})}{(\mu_1\mu_2\ldots\mu_{l-1})(\bar{\alpha}_1\bar{\alpha}_2\ldots\bar{\alpha}_l)} \cdot \frac{\bar{F}_1\bar{F}_2}{D\bar{T}D_0} \right\} du, \\ \bar{F}_1 &= [D\bar{T}D_m e^{\bar{\alpha}_m(d_m - h_1)} + D\bar{T}N_m e^{-\bar{\alpha}_m(d_m - h_1)}], \\ \bar{F}_2 &= [T\bar{D}D_{l-1}e^{\bar{\alpha}_1 h_2} + T\bar{D}N_{l-1}e^{-\bar{\alpha}_1 h_2}]. \end{aligned} \tag{2}$$

$$D\bar{T}D_i = (\mu_{i+1}\bar{\alpha}_i + \mu_i\bar{\alpha}_{i+1})D\bar{T}D_{i+1} + (\mu_{i+1}\bar{\alpha}_i - \mu_i\bar{\alpha}_{i+1})D\bar{T}N_{i+1}e^{-2\bar{\alpha}_{i+1}d_{i+1}}, \quad (4)$$

$$D\bar{T}N_N = 0, \quad (5)$$

$$D\bar{T}D_N = 1, \quad (6)$$

$$T\bar{D}D_{-1} = 1, \quad (7)$$

$$T\bar{D}N_{-1} = 0, \quad (8)$$

$$T\bar{D}D_{k-1} = (\mu_{k-1}\bar{\alpha}_k + \mu_k\bar{\alpha}_{k-1})T\bar{D}D_{k-2} + (\mu_{k-1}\bar{\alpha}_k - \mu_k\bar{\alpha}_{k-1})T\bar{D}N_{k-2}e^{-2\bar{\alpha}_{k-1}d_{k-1}}, \quad (9)$$

$$T\bar{D}N_{k-1} = (\mu_{k-1}\bar{\alpha}_k - \mu_k\bar{\alpha}_{k-1})T\bar{D}D_{k-2} + (\mu_{k-1}\bar{\alpha}_k + \mu_k\bar{\alpha}_{k-1})T\bar{D}N_{k-2}e^{-2\bar{\alpha}_{k-1}d_{k-1}}. \quad (10)$$

The coefficients described in (3)-(10) are determined by a recursive function dependent on earth layer and positions of conductor i and j, which determines integrate final form in (2).

For calculate self impedance of conductor i using (2), is just necessary set $m = l$ and replace the horizontal distance with cable outer radius and h_2 with h_1 [5].

The numerical solution for improper integral, presented in (2), is reported in [11], using adaptive quadrature.

C. Conductive coupling

The conductive coupling is a ground potential rise (GPR) caused by current injection into the soil by a transmission line or substation during fault condition which involves the earth, as shown in Fig. 3 [1].

The current flowing into earth through the transmission line grounding counterpoises produces a GPR, which appears in the form of voltage gradient around the grounding conductors. If a target structure is inside the region affected by the GPR, voltages may rise and be hazardous for the installation.

This EMI is influenced by short-circuit levels, quantity and type of shield wires, distance between the installations, grounding electrode geometry and soil resistivity [1].

Martins-Britto [12] proposed a circuit model for account conductive coupling in buried conductors using Green's function, proposed by He et al. [6] and Li et al. [7], which calculate a GPR in stratified soil. The circuit model considers a source voltage controlled by current connected to conductors coating impedance [12].

According to the principle of superposition, the ground potential rise U_P in a target point P caused by the sum of current injection I into soil in an observation point O_j, is given by [7]:

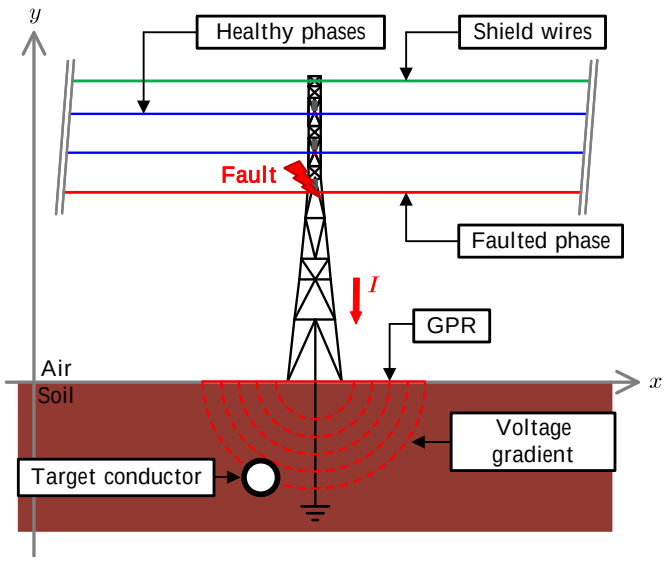

Fig. 3. Conductive coupling phenomenon, adapted from [12].

$$U_P = \sum_{j=1}^{N} \hat{G}(P, O_j) \cdot I_j, \quad (12)$$

in which U_P is the potential rise at target point P, in volts; O_j are the spatial coordinates of the j^{th} observation point O; and $\hat{G}(P, O_j)$ is a special function that describes the potential produced at point P by a unit point current source located at point O_j, known as Green's function [7], [12].

D. Green's function for N-layered soil

The Green's function in an earth structure with N horizontal layers is reported in [6], [7]. If the source point is located in the i^{th} layer and the observation point is in j^{th}, Green's function general form is written in (11), in which $r = \sqrt{(x_O - x_P)^2 + (y_O - y_P)^2}$ is the radius in xy plane; $z = z_O - z_P$ is the depth distance between point O and P; ρ_i is the resistivity of the i^{th} layer, in ohms.meter; $\hat{J}_0$ is the Bessel function of the first kind and order zero; and $\delta(ij)$ is the Kronecker delta, defined as equal to 1 if $i = j$ and to 0 otherwise [7].

Green's function coefficients $A_{i,j}$ and $B_{i,j}$ are determined by boundary conditions between surrounding earth layers, also air layer (0-layer) and deep layer (N-layer), as described in:

$$\hat{G}_{i,j}(r,z)|_{z=H_j-d} = \hat{G}_{i,j+1}(r,z)|_{z=H_j-d}, \quad (13)$$

$$\frac{1}{\rho_j}\frac{\partial \hat{G}_{i,j}(r,z)}{\partial z}\bigg|_{z=H_j-d} = \frac{1}{\rho_{j+1}}\frac{\partial \hat{G}_{i,j+1}(r,z)}{\partial z}\bigg|_{z=H_j-d}, \quad (14)$$

$$\hat{G}_{i,N}(r,z)|_{z\to\infty} = 0, \quad (15)$$

$$\frac{\partial \hat{G}_{i,0}(r,z)}{\partial z}\bigg|_{z\to\infty} = 0, \quad (16)$$

$$\hat{G}_{i,j}(P,O) = \frac{\rho_i}{4\pi}\left(\int_0^\infty A_{i,j}(\lambda)\hat{J}_0(\lambda r)e^{-\lambda z}d\lambda + \int_0^\infty B_{i,j}(\lambda)\hat{J}_0(\lambda r)e^{\lambda z}d\lambda + \int_0^\infty \delta(ij)\hat{J}_0(\lambda r)e^{-\lambda|z|}d\lambda\right) \quad (11)$$

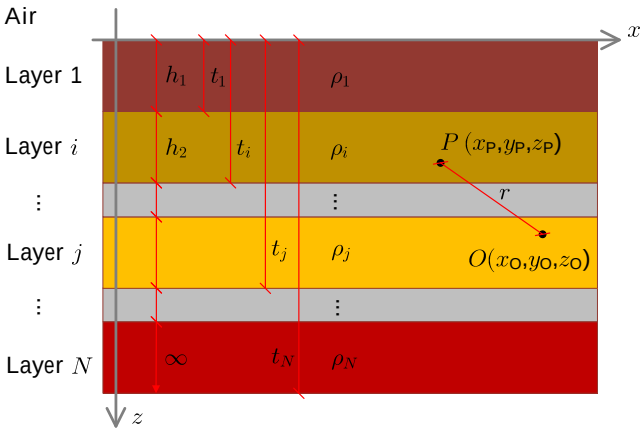

Fig. 4. Point source at i^{th} layer with observation point at j^{th}.

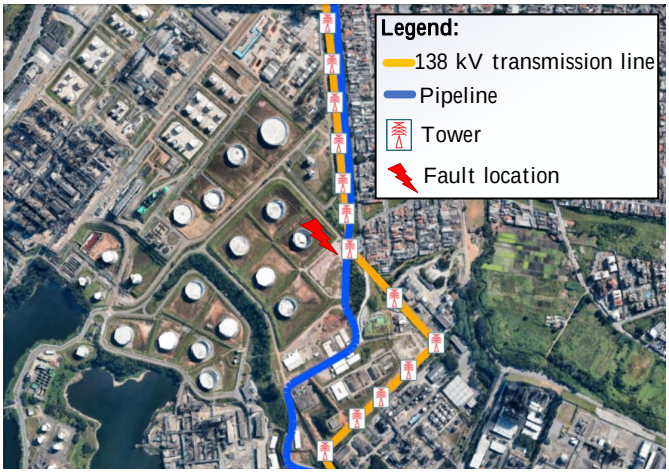

Fig. 5. Shared right-of-way between transmission line and pipeline in Brazil.

in which $i = 1, 2, \ldots, N$ and $H_0 = 0$.

E. Stress voltage

The target conductor located on earth and nearby a transmission line is subjected to two distinct electromagnetic influences under fault conditions. The total voltage transferred to the interfered conductor is the potential difference between the voltage caused by inductive coupling and by conductive coupling, or [13]:

$$V_S = E_T - U_P, \quad (17)$$

in which V_S is the total stress voltage, in volts; E_T is the potential of the target conductor resulting from inductive coupling, in volts; and U_P is the local earth potential rise, in volts.

III. Description of the Real Case Scenario

Fig. 5 illustrates a 1.2 km shared right-of-way composed by a 138 kV transmission line and an underground pipeline, in an industrial area of São Paulo, Brazil. Under nominal load condition, the double-circuit transmission line is energized with ABC/ABC sequence, 60 Hz frequency and current of 780 A per phase. In the path analyzed, the transmission line is constituted of 13 towers, which each is grounded through 15 Ω electrodes, and 2 substations in extremities, which each is grounded through 1 Ω electrodes. The transmission line side view and the conductor coordinates are presented in Fig. 6.

The underground pipeline is constructed in 14" diameter carbon steel and is located in 1.2 meters above ground. The pipeline is grounded in its extremities through 10 Ω resistances. The characteristics of transmission line conductors and the pipeline are presented in Table I.

The soil is modeled in a 3-layer structure based on apparent resistivities measurements in the right-of-way location. The

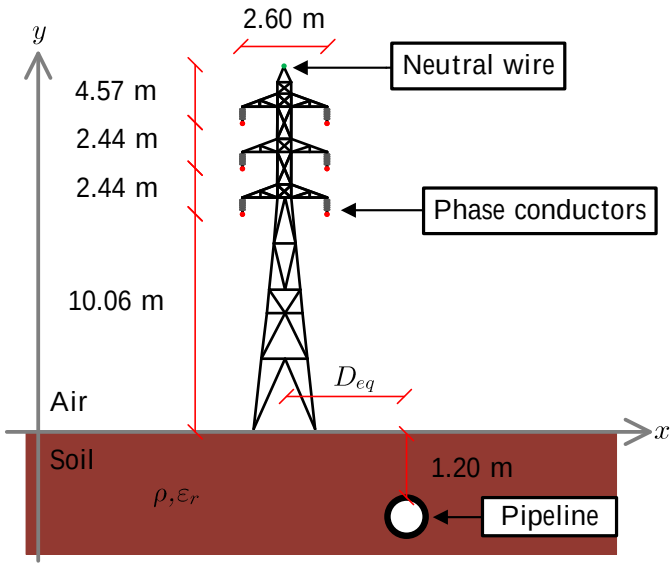

Fig. 6. System geometry.

specifications of the layers resistivities and thickness are presented in Table II.

IV. Real Case Study Under Nominal Load Conditions

A. Nominal load EMTP equivalent circuit

Due to the shared right-of-way is composed of obliquities, crossings and parallelisms, the right-of-way is subdivided and, for each subdivided segment, is calculated a parallalel equivalent segment, as described in detal in [14]. The transmission line is modeled as a series of Line Constants (LCCs) blocks, in

TABLE I
SPECIFICATION AND CHARACTERISTICS OF SYSTEM CONDUCTORS

Conductor	r_{out} [m]	r_{in} [m]	$R_{DC}[\Omega/km]$
ACSR Grosbeak	0.0125705	0.0046355	0.0924806
Steel 3/8" EHS-CG	0.004572	-	3.42313
Pipe 14"	0.1778	0.168275	0.099516

TABLE II
SOIL PARAMETERS

Layer	Resistivity [Ω.m]	Thickness [m]
1	488.71	1.73
2	2074.66	8.99
3	451.41	∞

which is inserted the parallel segment parameters, respectively. Fig. 7 presents the simplified circuit for nominal load simulation, which source of Transient Analysis of Control Systems (TACS) represents sum of the EMFs in phase conductors and shield wires. The current probe of TACS is placed to measure current in each LCC out and the current values are used to build EMFs sources in the interfered conductor, represented in the inferior part of Fig. 7.

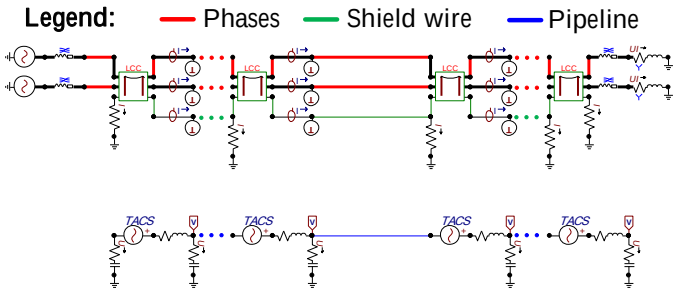

Fig. 7. Nominal load EMTP simplified model representation.

It is important to notice that this proposed model do not consider the interferences in the transmission line caused by the pipeline coupling influences. However, a low current flows along pipeline compared to the transmission line currents, then the pipeline influences on transmission line is considered negligible.

B. Nominal load simulation results

Fig. 8 shows induced voltage along the pipeline using the proposed model, as well as comparative responses with the EMI reference software CDEGS [15].

Results shows that the proposed model agreed with the reference software, presenting a 7.35% normalized root-mean-square deviation (NRMSD).

Due to the grounding resistance in pipeline extremities, the induced voltage do not exceed the safety limit of 15 V in steady-state regime [16]. Grounding resistances provides a safe path to the induced currents to earth, which prevent risks to the interfered installation.

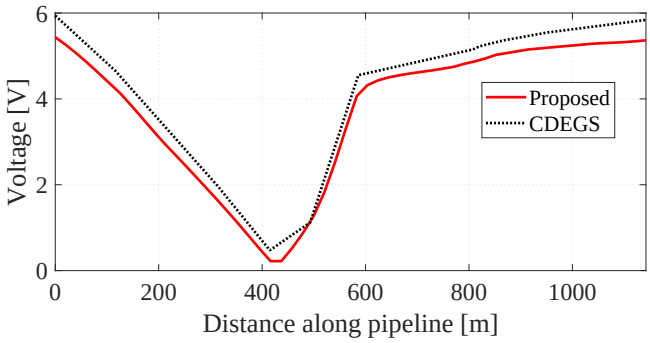

Fig. 8. Induced voltage along pipeline under nominal load conditions.

V. REAL CASE STUDY UNDER FAULT CONDITIONS

In order to study the ground potential rise and total stress voltage, is applied a phase-to-ground fault to the system presented in Section III.

A. Fault regime EMTP equivalent circuit

The transient regime is caused by a phase-to-ground fault located at 7# tower. A 0.001 Ω resistance value is chosen to represent a short-circuit between the phase B conductor and earth.

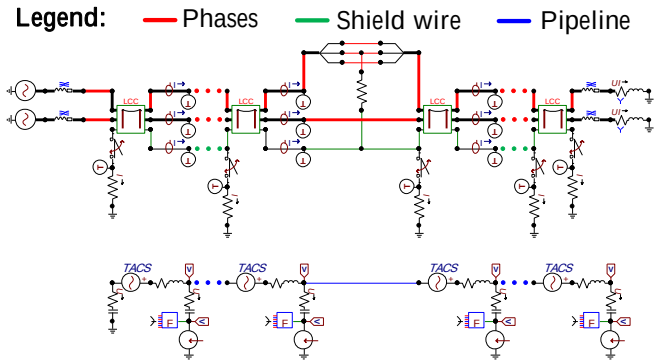

Fig. 9. EMTP simplified model representation for fault regime study.

Fig. 9 shows the simplified equivalent circuit for fault conditions. The model is constructed as in nominal load condition, described in the previous section. However, others sources of TACS are connected to the pipeline coating impedance to represent the ground potencial rise due to the conductive coupling. The current probe of TACS measure the current flowing through each tower grounding impedance to earth.

B. Results from fault conditions simulation

The total stress voltage, the potential resulting from inductive coupling and the local earth potential rise due to the phase-to-ground fault are presented in Fig. 10.

The obtained results for ground potential rise and total stress voltage agreed with the reference software, with 1.42% and

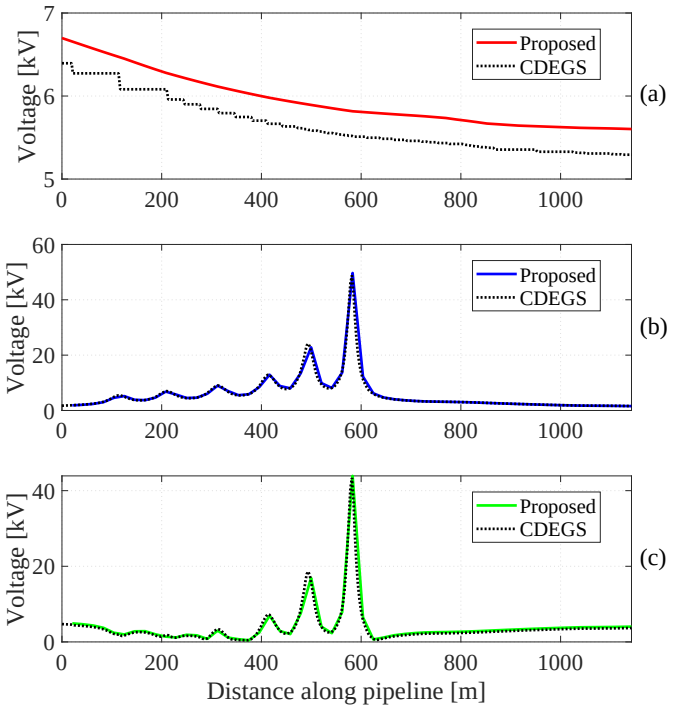

Fig. 10. Pipeline voltage due to: (a) inductive coupling; (b) GPR; and (c) total stress.

1.21% of NRMSD, respectively. The induced voltage presented 21.17% of deviation. However, measure the deviation from relative error is more appropriated due to the voltage behavior tend to a constant value. Considering relative error, the induced voltage presented a deviation of 5.5%.

The total stress voltage along the pipeline reaches 43.9 kV nearby fault location, which may cause breakdown of the dielectric of the coating layer, exposing the metal to electrochemical corrosion [16]. Modern pipeline coatings are designed to withstand a voltage limit of 25 kV [16].

The currents flowing to shield wire and to the ground through tower grounding are shown in Fig. 11. The higher currents are presented in the faulted tower (7# tower). Great values of voltage are observed in virtue of the magnitudes of short-circuit contribution currents, as well as the currents injected to the soil provides the potential rise to the nearby pipeline.

VI. Mitigation Study

As the total stress in steady-state fault regime extrapolated standard limits, which may present risks to the pipeline coating, a mitigation strategy is proposed. The proposed mitigation consists of connect the pipeline in specific points to the earth through grounding electrodes with low resistances values ($\leq 10\ \Omega$). This method is used to transfer the ground potential rise to the metal pipe, then the difference in (17) will reduce and, consequently, the total stress in this specific points will reduce.

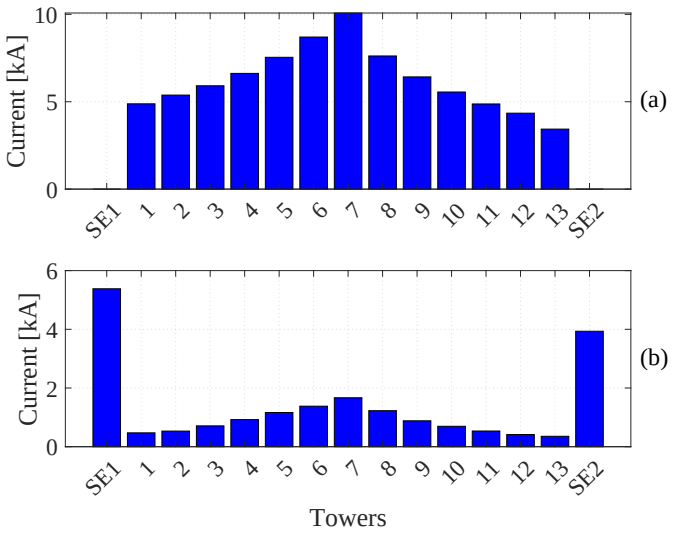

Fig. 11. (a) Grounding currents; and (b) currents flowing in the shield wire.

In the case present in this paper, the hazardous region is located at 450 to 650 meters on the pipeline path. In the hazardous region, for each 40 meters is connected a 1 Ω grounding resistance between the pipeline and earth, resulting 5 electrodes in total. Fig. 12 present the comparison between the pipeline voltages after and before mitigation.

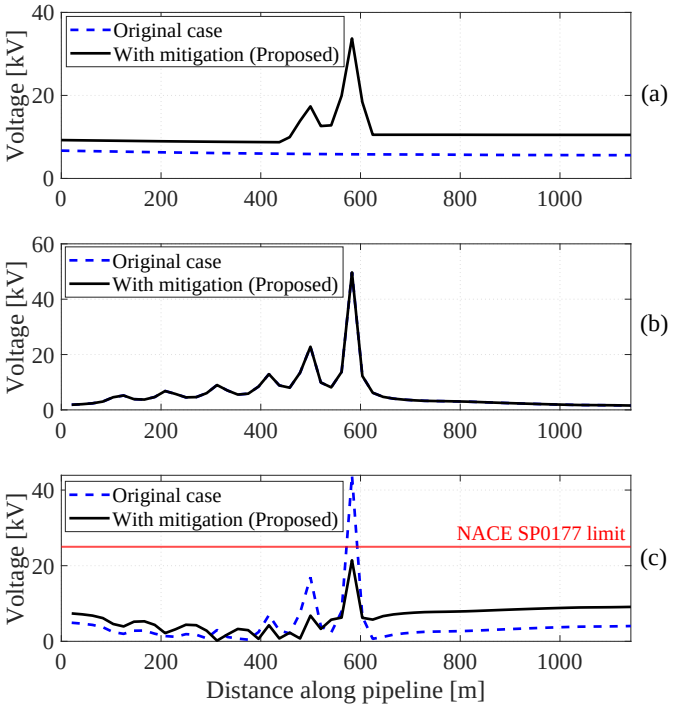

Fig. 12. Comparison of pipeline voltages after and before mitigation due to: (a) inductive coupling; (b) GPR; and (c) total stress.

Is observed that the proposed mitigation reduce the stress

voltage to 21 kV meeting the safety criteria adopted in pipeline industry [16].

It is important to notice that the mitigation method decreases the stress voltages in intended location. However, in regions out of the mitigation the potential in the pipeline rises. Also, the induced voltage due to inductive coupling reaches 33 kV, approximately 6.6 times superior to the original case.

Then, obtained responses using the mitigation strategy discussed is valid, although is interesting known that this strategy implies other complications and its may be lead to other hazardous situations to the installation and people involved.

VII. Conclusions

This work presents a EMTP-based circuit approach to predict total stress voltage in a pipeline due to a transmission line phase-to-ground fault. The proposed method is based on formulations which considers multilayered soils without approximations or uniform equivalents.

To validate the proposed methodology, a real shared right-of-way composed of an underground pipeline and a double-circuit 138 kV transmission line is modeled, under nominal conditions and fault conditions.

Results show that the methodology is valid and accurated under both nominal and fault conditions, presenting 7.35% of deviation compared to an electromagnetic influences industry-standard software.

Under nominal conditions, peak of induced voltage reaches 6 V and its considered a safe value to the facilities and employees involved. However, in steady-state fault regime, the stress voltage reaches 43 kV, which may be hazardous for the pipeline coating and disagree with the nominal limits established for the industry.

For this reason, further studies is simulated and a mitigation is designed to the real case presented. The method consisted in connect grounding electrodes in the region of the pipeline which reaches hazardous values. The results obtained proved that the mitigation method is valid, which decreased 47% of the peak values leading the stress voltage under to the 25 kV safe limit. However, is important to notice that this mitigation method rises the stress voltage out of the mitigated region, which may implies in others hazardous situations.

References

[1] CIGRÉ WG-36.02, "Technical Brochure n. 95 - Guide on the Influence of High Voltage AC Power Systems on Metallic Pipelines," Paris, pp. 1–135, 1995.

[2] L. Qi, H. Yuan, L. Li, and X. Cui, "Calculation of Interference Voltage on the Nearby Underground Metal Pipeline due to the Grounding Fault on Overhead Transmission Lines," *IEEE Transactions on Electromagnetic Compatibility*, vol. 55, no. 5, pp. 965–974, 2013.

[3] X. Wu, H. Zhang, and G. G. Karady, "Transient analysis of inductive induced voltage between power line and nearby pipeline," *International Journal of Electrical Power and Energy Systems*, vol. 84, no. January, pp. 47–54, 2017. [Online]. Available: http://dx.doi.org/10.1016/j.ijepes.2016.04.051

[4] M. Alexandru, L. Czumbil, D. D. Micu, and T. Papadopoulos, "Analysis of Electromagnetic Interferences between AC High Voltage Power Lines and Metallic Pipeline Using Two Different Approaches Based on Circuit Theory and Electromagnetic Field Theory," *EPE 2020 - Proceedings of the 2020 11th International Conference and Exposition on Electrical And Power Engineering*, pp. 519–524, 2020.

[5] D. A. Tsiamitros, G. K. Papagiannis, P. S. Dokopoulos, and A. E. F. Equations, "Earth Return Impedances of Conductor Arrangements in Multilayer Soils - Part I : Theoretical Model," *IEEE Transactions on Power Delivery*, vol. 23, no. 4, pp. 2392–2400, 2008.

[6] J. He, R. Zeng, and B. Zhang, *Methodology and Technology for Power System Grounding*. Wiley, 2012.

[7] Z.-X. Li, J.-B. Fan, and W.-J. Chen, "Numerical simulation of substation grounding grids buried in both horizontal and vertical multilayer earth model," *International Journal for Numerical Method in Engineering*, no. February, pp. 1102–1119, 2006. [Online]. Available: http://onlinelibrary.wiley.com/doi/10.1002/nme.3279/full

[8] J. R. Carson, "Wave Propagation in Overhead Wires with Ground Return," *Bell System Technical Journal*, vol. 5, no. 4, pp. 539–554, 1926.

[9] M. Nakagawa, A. Ametani, and K. Iwamoto, "Further Studies on Wave Propagation in Overhead Lines with Earth Return: Impedance of Stratified Earth," *Proceedings of the Institution of Electrical Engineers*, vol. 120, no. 12, p. 1521, 1973. [Online]. Available: https://digital-library.theiet.org/content/journals/10.1049/piee.1973.0312

[10] F. Pollaczek, "On the Field Produced by an Infinitely Long Wire Carrying Alternating Current," *Electrische Nachrictentechnik*, vol. III, no. 9, pp. 339–359, 1926.

[11] L. F. Shampine, "Vectorized adaptive quadrature in MATLAB," *Journal of Computational and Applied Mathematics*, vol. 211, no. 2, pp. 131–140, 2008.

[12] A. G. Martins-Britto, "Realistic Modeling of Power Lines for Transient Electromagnetic Studies," Ph.D. dissertation, University of Brasília, 2020. [Online]. Available: https://www.researchgate.net/publication/342916469_Realistic_Modeling_of_Power_Lines_for_Transient_Electromagnetic_Interference_Studies

[13] IEEE Std 80, "Guide for Safety In AC Substation Grounding," pp. 1–192, 2000.

[14] C. M. Moraes, A. G. Martins-Britto, and F. V. Lopes, "Electromagnetic Interferences Between Power Lines and Pipelines Using EMTP Techniques," *WCNPS 2020: 5th Workshop on Communication Networks and Power Systems*, 2020.

[15] F. Dawalibi and C. Blattner, "Earth Resistivity Measurement Interpretation Techniques," *IEEE Transactions on Power Apparatus and Systems*, vol. PAS-103, no. 2, pp. 374–382, 1984. [Online]. Available: http://ieeexplore.ieee.org/lpdocs/epic03/wrapper.htm?arnumber=4112522

[16] NACE International, *Mitigation of Alternating Current and Lightning Effects*, 2007, vol. SP0177.